Heliospheric energetic particle observations during the October–November 2003 events

D. Lario, R. B. Decker, S. Livi, S. M. Krimigis, and E. C. Roelof
Johns Hopkins University Applied Physics Laboratory, Laurel, Maryland, USA

C. T. Russell
Department of Earth and Space Sciences, Institute of Geophysics and Planetary Physics, University of California, Los Angeles, California, USA

C. D. Fry
Exploration Physics International, Inc., Huntsville, Alabama, USA

Received 30 November 2004; revised 11 April 2005; accepted 21 April 2005; published 4 August 2005.

[1] The intense level of solar activity recorded from 19 October to 12 November 2003 led to unusually high energetic particle intensities observed throughout the heliosphere. The fleet of spacecraft distributed in the inner and outer heliosphere offers us the opportunity to study both the effects of these events in different regions of the heliosphere and the evolution of the energetic particle intensities measured at different heliocentric radial distances. Observations at 1 AU by the ACE and GOES-11 spacecraft show multiple particle intensity enhancements associated with individual injections of solar energetic particles (SEPs) and with the arrival of shocks driven by coronal mass ejections (CMEs), resulting in a long time interval ($\sim$40 days) of elevated low-energy (<1 MeV) ion and near-relativistic (<315 keV) electron intensities. Observations from the Ulysses spacecraft at 5.2 AU, 6° north of the ecliptic, and 120–90° west of the Earth also showed elevated low-energy ion and near-relativistic electron intensities for more than $\sim$40 days that were modulated by the effects of recurrent corotating interaction regions (CIRs) and the passage of a fast interplanetary coronal mass ejection (ICME). The Cassini spacecraft at 8.7 AU, 3° south of the ecliptic, and 75–35° west of the Earth saw an intense low-energy ion and near-relativistic electron event in association with the passage of an enhanced magnetic field structure formed by the compression of transient solar wind flows and CIRs. The prompt component of the SEP event at Cassini was largely reduced due to the modulating effect of intervening transient flows propagating between the Sun and the spacecraft. The Voyager-2 spacecraft at 73 AU and 25° south of the ecliptic did not observe these events until April 2004. The arrival of a merged interaction region (MIR) at Voyager-2 produced a $\sim$70-day period with elevated <17 MeV proton and <60 keV electron intensities. Particle fluences computed over the duration of the events at each spacecraft show a radial dependence that decays more slowly than that expected from a simple model assuming adiabatic cooling of an isotropic particle population uniformly distributed in a shell symmetrically expanding at the solar wind speed. Although the SEP events were observed throughout the heliosphere, both (1) the solar particle injections occurring at different times and longitudes, and (2) the marked differences in the interplanetary stream structures propagating toward different longitudes resulted in distinct time-intensity histories at each spacecraft, and therefore periods with equal particle intensities were not observed by this fleet of spacecraft.

Citation: Lario, D., R. B. Decker, S. Livi, S. M. Krimigis, E. C. Roelof, C. T. Russell, and C. D. Fry (2005), Heliospheric energetic particle observations during the October–November 2003 events, *J. Geophys. Res.*, *110*, A09S11, doi:10.1029/2004JA010940.

1. Introduction

[2] After a quiescent period of two months without any significant major solar event, the series of intense solar flares and fast coronal mass ejections (CMEs) observed in late October and early November 2003 not only impressed the space physics community [*Irion*, 2004] but also strongly affected different regions of the heliosphere [*Lopez et al.*, 2004]. The associated solar energetic particle (SEP) events were some of the largest in solar cycle 23 as observed in the

0148-0227/05/2004JA010940$09.00

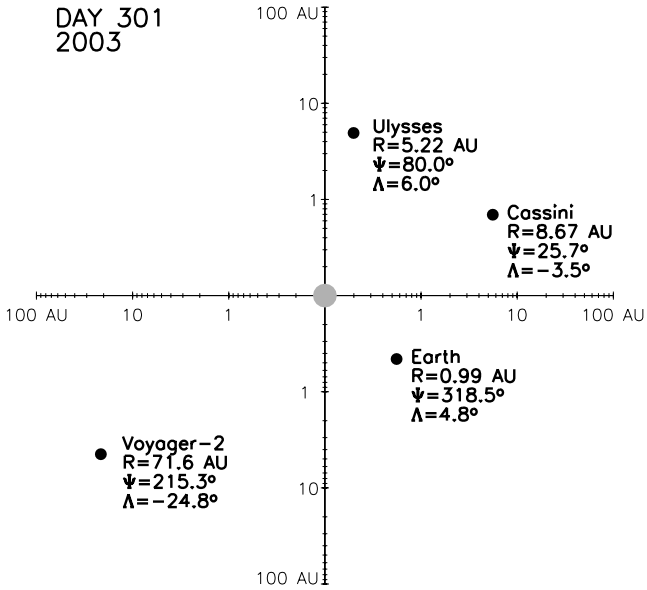

Figure 1. Locations of Earth, Ulysses, Cassini, and Voyager-2 on 28 October 2003 (day 301).

ecliptic plane at the heliocentric distance of 1 AU [*Cohen et al.*, 2005]. This series of events occurred 3.5 years after the peak month (April 2000) of the sunspot maximum of solar cycle 23, i.e., during the declining phase of the solar activity cycle [*Dryer et al.*, 2004]. Although large SEP events are more frequent during the maximum of solar activity, major SEP events can occur at any time during the solar cycle, especially in its declining phase [*Shea and Smart*, 2001]. That was the case of the well-studied SEP events in August 1972 and October–November 1992 [e.g., *Lario and Simnett*, 2004] and it is again the case of the October–November 2003 events.

[3] From 19 October 2003 (day of year 292) to 5 November 2003 (day of year 309), 44 M-class and 11 X-class flares were observed [*Woods et al.*, 2004] coinciding with the transit of the NOAA active regions AR 0484, 0486, and 0488 over the disk of the Sun. The intense level of solar activity continued after these active regions crossed the west limb of the Sun [*de Koning et al.*, 2005]. The interplanetary consequences of these series of events extended over an even longer time interval. The system of transient interplanetary flows generated by this series of events expanded within the heliosphere arriving separately at the locations of the spacecraft distributed over the heliosphere [*Richardson et al.*, 2005].

[4] The purpose of this paper is to document the physical consequences of these extreme events in terms of the energetic particle intensities measured by the current fleet of heliospheric spacecraft. We present energetic particle data measured by the spacecraft located in the inner heliosphere ($\lesssim$10 AU) from 20 October 2003 (day of year 293) to 2 December 2003 (day of year 336). These spacecraft include ACE, GOES-11, Ulysses, and Cassini. For those spacecraft in the outer heliosphere (in this case we only include Voyager-2) we analyze energetic particle data from 30 March 2004 (day of year 90) to 23 June 2004 (day of year 175). Figure 1 shows the locations of the spacecraft at the time of the X17 flare on 28 October 2003 (day of year 301). This flare was associated with the origin of the most intense SEP event observed at 1 AU during this time interval [*Cohen et al.*, 2005]. The ACE spacecraft, in orbit around the L1 Sun-Earth libration point, and the GOES-11 spacecraft, in geosynchronous orbit, are too close to the Earth to be plotted separately in Figure 1. All the spacecraft considered in this study were at low heliographic latitudes ($\Lambda < \pm 6°$), with the exception of Voyager-2 that was at $\Lambda = -25°$. The range of inertial heliographic longitudes (Ψ) embraced by these spacecraft on day 301 was 104° east of the Earth and 122° west of the Earth, with the Earth (together with the ACE and GOES-11 spacecraft) moving westward at the rate of $\sim$1° per day and the rest of spacecraft maintaining approximately the same inertial heliographic longitude throughout the period considered in this paper.

[5] Multispacecraft observations of SEP events by widely separated observers are difficult to interpret because of the variety of processes involved in the development of the SEP events. This is particularly true when the spacecraft are beyond 1 AU because (1) particle transport effects become the dominant factor in shaping the observed time-intensity profiles, (2) multiple particle injections at the Sun tend to occur in periods of intense solar activity when several CMEs occur sequentially in a short time interval, making the identification of the particle sources ambiguous, and (3) the particle intensities are modulated by traveling interplanetary structures en route between the particle sources and the observer. These transient structures are able to channel, confine, and reaccelerate energetic particles, modifying the characteristics of the SEP events measured beyond 1 AU. A description of these processes and their effects in the development of SEP events at distances beyond 1 AU can be found in the works of *Lario et al.* [2000a, 2004a].

[6] In this paper, we first analyze the large-scale structure of the inner heliosphere ($\lesssim$10 AU) prior to the occurrence of the October–November 2003 events in order to establish the conditions under which these events occurred. In section 3 we present the energetic particle observations at 1 AU, Ulysses, Cassini, and Voyager-2 and discuss the causes of the different time-intensity profiles observed at each spacecraft. In section 4, we discuss the longitudinal and radial dependence of both the time-intensity histories and the particle fluences integrated over the duration of the events. Finally, in section 5 we summarize the main results of this work.

2. Preevent and Postevent Structure of the Heliosphere

[7] The inner heliosphere prior to 19 October 2003 (day of year 292) was typical of the declining phase of the solar cycle [*Jackman et al.*, 2004]. Figure 2 shows solar wind and interplanetary magnetic field (IMF) data from ACE and Ulysses (Figures 2a and 2b) as well as IMF data from the Cassini spacecraft (Figure 2c) from 18 August 2003 (day 230) to 5 January 2004 (day 370). Magnetic field observations were made by the Magnetic Fields Experiment (MAG) on ACE [*Smith et al.*, 1998], the Vector Helium Magnetometer (VHM) sensor on Cassini [*Dougherty et al.*, 2004], and the VHM on Ulysses [*Balogh et al.*, 1992]. The angular

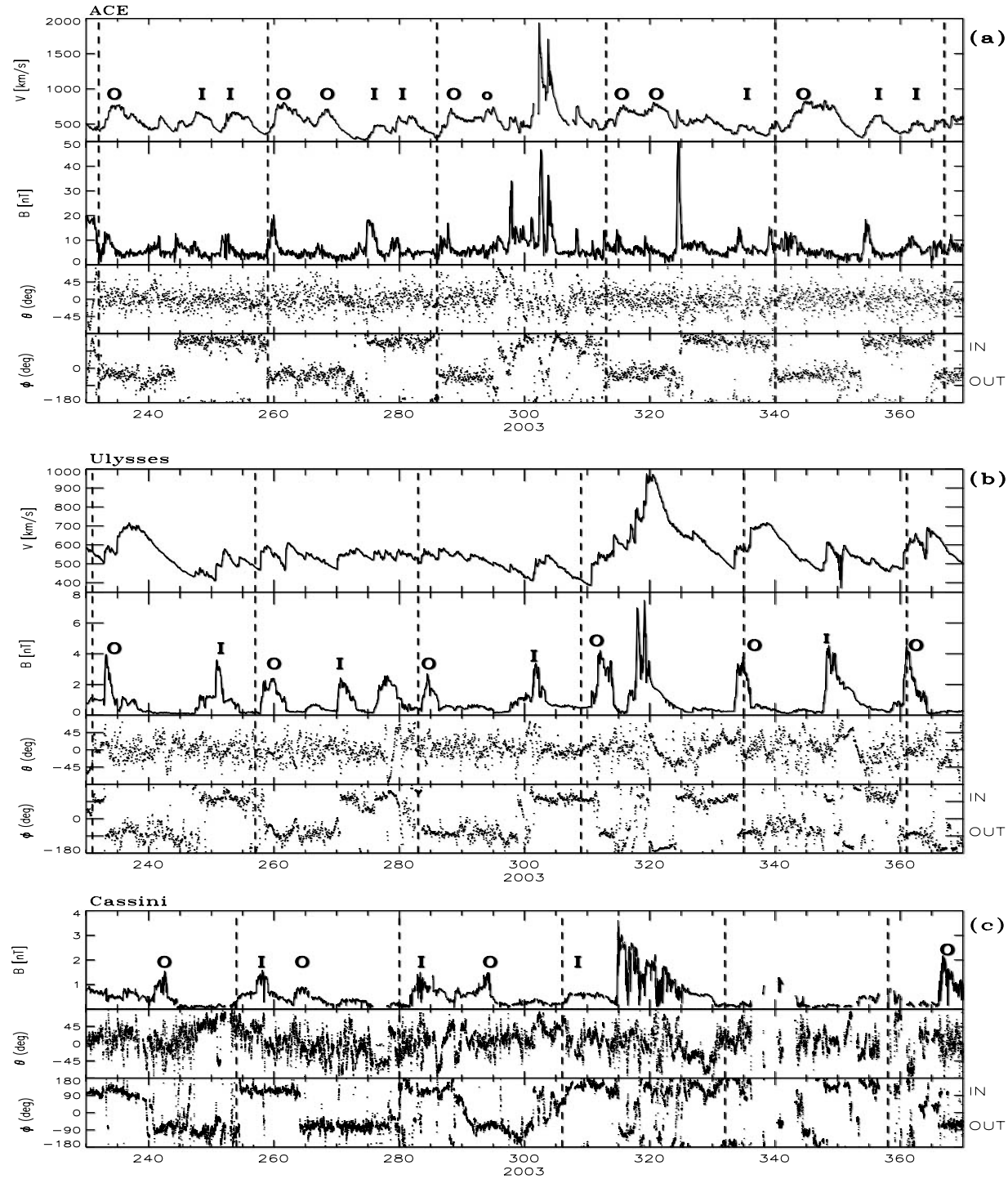

Figure 2. (a) Hourly averages of the solar wind speed measured by the SWEPAM instrument on board ACE [*McComas et al.*, 1998], magnetic field magnitude and orientation (in the RTN coordinate system) as measured by the MAG instrument on board ACE [*Smith et al.*, 1998]. (b) Hourly averages of the solar wind speed measured by the SWOOPS instrument on board Ulysses [*Bame et al.*, 1992], magnetic field magnitude and orientation (in the RTN spacecraft centered coordinate system) as measured by the VHM instrument on board Ulysses [*Balogh et al.*, 1992]. (c) 10-min averages of the magnetic field magnitude and orientation (in the RTN spacecraft centered coordinate system) as measured by the VHM instrument on board Cassini [*Dougherty et al.*, 2004]. The dashed vertical lines are spaced 27 days apart in Figure 2a and 26 days apart in Figures 2b and 2c. The symbols **O** and **I** identify in Figure 2a the high-speed solar wind streams with outward and inward magnetic polarities, respectively, whereas in Figures 2b and 2c they identify the associated CIRs.

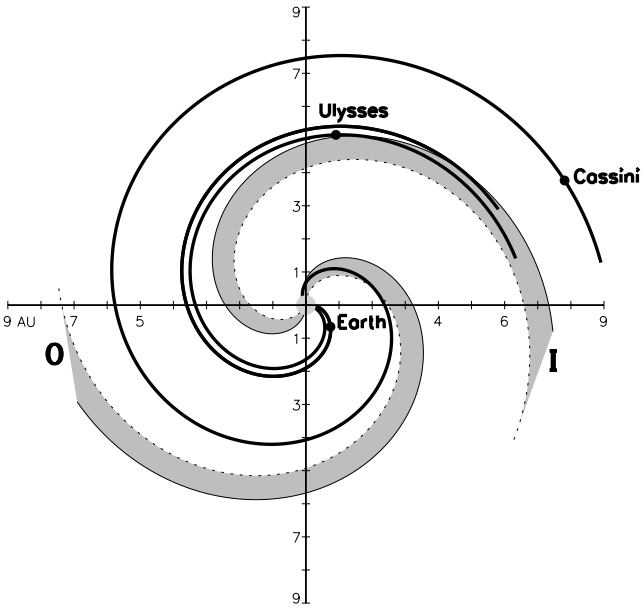

Figure 3. Schematic representation of the ecliptic plane prior to the occurrence of the events in late October 2003. The solid lines represent nominal IMF lines connecting each spacecraft with the Sun, and the gray areas represent the outward polarity (**O**) and inward polarity (**I**) CIRs recurrently observed in the inner heliosphere prior to the events.

directions (θ, ϕ) of the IMF are given in the RTN spacecraft centered coordinate system defined in Figure 1 of *Forsyth et al.* [1995]. Solar wind speeds were measured by the Solar Wind Electron Proton Alpha Monitor (SWEPAM) on ACE [*McComas et al.*, 1998] and the Solar Wind Plasma experiment (SWOOPS) on Ulysses [*Bame et al.*, 1992]. SWEPAM data from day 301 to 304 exist only in a ~33 min time resolution [*Skoug et al.*, 2004]. Unfortunately, solar wind plasma parameters at Cassini were not available for most of the period considered because of limitations imposed by the spacecraft pointing direction.

[8] The dashed vertical lines plotted in Figure 2 indicate the solar rotation period (27 days apart in Figure 2a for near-Earth spacecraft to account for the Earth's motion and 26 days apart in Figures 2b and 2c for those spacecraft further out in the heliosphere). With the exception of the time interval when the transient flow system generated by the October–November 2003 events passed over each one of the spacecraft [*Richardson et al.*, 2005], two magnetic field sectors were observed in each solar rotation [*Jackman et al.*, 2004]. Recurrent high-speed (~600 km s^{-1}) streams dominated the structure of the inner heliosphere. Magnetic field compression regions were clearly observed by Ulysses at ~5 AU and Cassini at ~8 AU.

[9] We have identified in Figure 2 the successive appearance of the high-speed streams and associated corotating interaction regions (CIRs). The symbols **O** and **I** indicate the magnetic field sector measured during the high-speed solar wind stream generating the CIR (**O** for outward directed field and **I** for inward magnetic field). A schematic representation of the large-scale structure of the inner heliosphere before the occurrence of the October–November 2003 events is shown in Figure 3. The solid lines show the nominal Parker field lines magnetically connecting each spacecraft with the Sun. The two inward polarity (**I**) and outward polarity (**O**) compression regions are represented by the gray areas.

[10] The recurrent structure of high-speed streams with different magnetic field polarities was disrupted by the passage of the transient events (see Figure 2). The inward polarity high-speed streams expected to be observed by ACE during the time interval of the October–November 2003 events were not easily identifiable. Similarly, the inward polarity CIR expected at Ulysses during the rotation on days 309–335 was not clearly distinguishable in the wake of the fast ICME observed by Ulysses on days 320–324 [*de Koning et al.*, 2005]. The outward polarity CIR expected at Cassini during the rotation on days 306–332 cannot be identified due to the passage of an enhanced transient magnetic field structure.

[11] The two sector magnetic field structure quickly recovered in the rotation following the passage of the transient flows as seen by ACE and Ulysses when the recurrent structure of CIRs emerged again (Figures 2a and 2b). Gaps in the Cassini magnetic field data do not allow us to discern the two sector magnetic field structure during the rotation on days 332–358 at Cassini (Figure 2c); however, it was clearly observed in the following rotations as shown in Figure 3 of the work of *Jackman et al.* [2004]. We should also note the detection of at least one isolated ICME by ACE on day 324, and of two additional ICMEs by Ulysses on days 278–280 and 350–353, as shown by the smooth magnetic field rotations in Figure 2.

3. Energetic Particle Observations

3.1. 1 AU Observations

[12] Figure 4 displays energetic particle data collected by the ACE and GOES-11 spacecraft from 20 October 2003 (day 293) to 2 December 2003 (day 336). Figures 4a and 4b show near-relativistic electron and low-energy ion intensities as measured by the EPAM instrument on board ACE [*Gold et al.*, 1998], whereas the Figure 4c shows proton intensities observed by the Energetic Particle Sensor (EPS) on board GOES-11 [*Sauer*, 1993]. Figure 4d shows the IMF magnitude as measured by the MAG magnetometer on board ACE [*Smith et al.*, 1998]. The solid vertical lines indicate the passage of interplanetary shocks and gray vertical bars the passage of the ICMEs. Table 1 lists the arrival time of the shocks and the start and end times of the ICME passages. We have identified the passage of interplanetary shocks and ICMEs following the work of *Skoug et al.* [2004]. *Malandraki et al.* [2005] analyzed also the energetic particle and magnetic field signatures associated with the passage of the ICMEs during this period. These signatures included bidirectional ~2 MeV ion flows (BIFs), bidirectional near-relativistic electron flows, low-variance magnetic field magnitude, smooth magnetic field rotations, and in some cases low-energy ion intensity depressions. All these signatures are typical of the passage of ICMEs in the ecliptic plane and at 1 AU from the Sun [*Richardson*, 1997; *Neugebauer and Goldstein*, 1997]. In Table 1 we have indicated the start and end times of the ICMEs inferred from the analysis of these signatures that differ from the

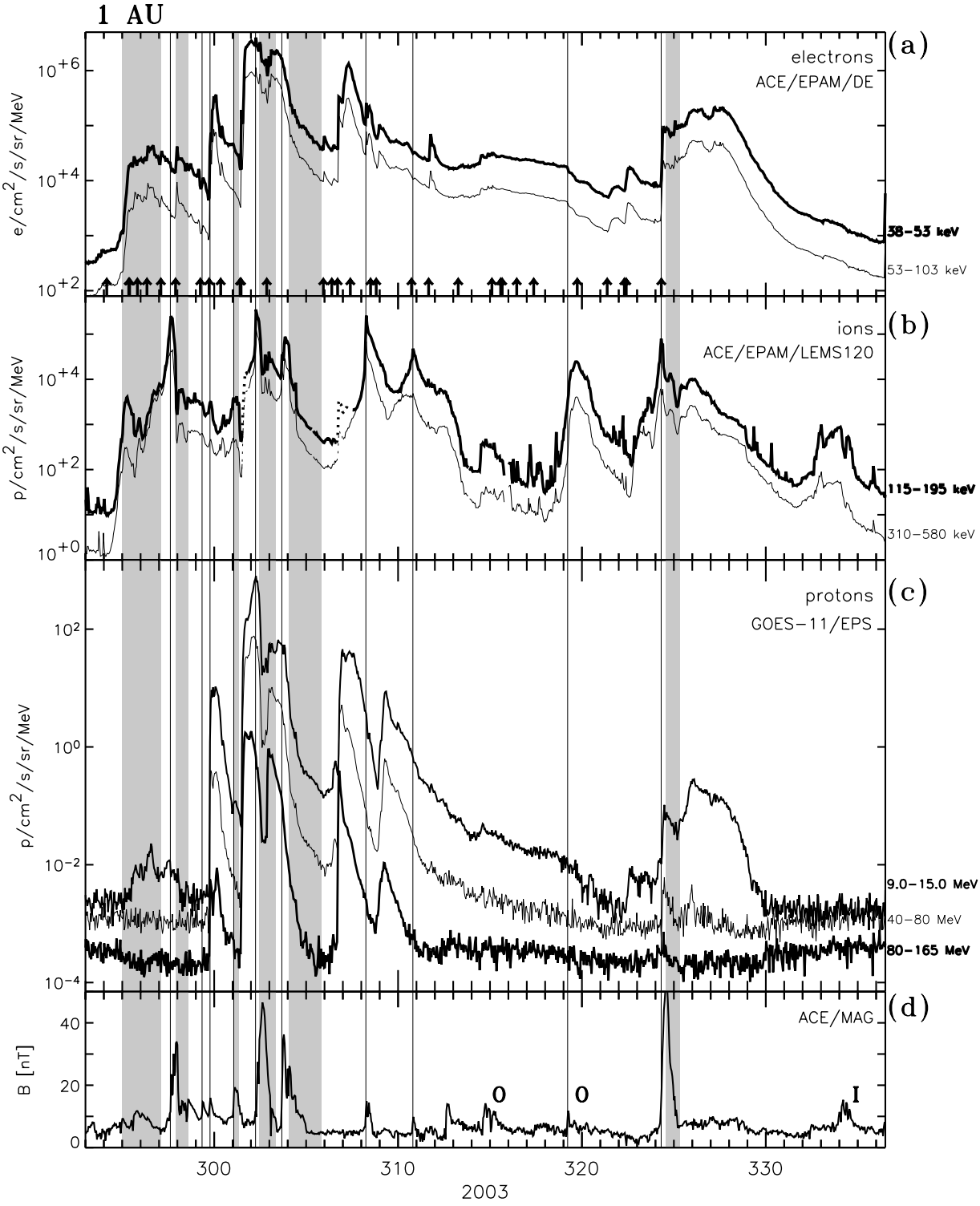

Figure 4. Hourly averages of the spin-averaged (a) electron, (b) ion, and (c) proton intensities measured by EPAM/DE on board ACE [*Gold et al.*, 1998], EPAM/LEMS120 on board ACE [*Gold et al.*, 1998] and the EPS on board GOES-11 [*Sauer*, 1993], respectively. Vertical arrows in Figure 4a indicate the solar events listed in Table 2. Dotted traces in the EPAM/LEMS120 ion time-intensity profiles indicate the time intervals with possible electron contamination. (d) Hourly averages of the magnetic field magnitude as measured by MAG on board ACE [*Smith et al.*, 1998]. Solid vertical lines and gray vertical bars indicate the passage of interplanetary shocks and ICMEs listed in Table 1. The Earth's inertial heliographic longitude varied from $\Psi = 310.6°$ on day 293 to $\Psi = 353.6°$ on day 336.

Table 1. Interplanetary Shocks and ICMEs

Shock Time	Start ICME	End ICME
	ACE[a]	
-	294/2330	297/0230[b]
297/1448	297/2200	298/1400
299/0809	-	-
299/1832	-	-
301/0131	301/0230	301/0830[c]
302/0558	302/1100	303/0855[b]
303/1619	304/0155	305/2150[b]
308/0559	-	-
310/1919	-	-
319/0519	-	-
324/0727	324/1100	325/0100
	Ulysses	
297/1711	-	-
-	298/2110	299/2025
301/0823	-	-
303/0756[d]	-	-
310/1648[e]	311/0245	312/2000[e]
311/1731[e]	-	-
314/0508[d,e]	-	-
316/0854[e]	-	-
317/1615[e]	317/2306	318/1050[e]
319/0033[e]	319/2010	324/0400[e]
326/2116[e]	-	-
333/1235	-	-
336/0123[d]	-	-
	Cassini	
314/1850[f]		
320/2200[d,f]		
-	325/0000	330/0000[g]
	Voyager-2	
119/0000[h]	Formation of a MIR[i]	

[a]Shock parameters and ICME identification at ACE can be found in the work of *Skoug et al.* [2004].

[b]ICME boundaries different from those identified by *Skoug et al.* [2004] and based on low-variance magnetic field rotations and energetic particle signatures. Evidences of ~2 MeV BIFs were observed from 295/1355 UT to 296/1424 UT, 302/1100 UT to 303/0855 UT, and 304/0200 UT to 305/1300 UT (see details in the work of *Malandraki et al.* [2005]).

[c]Low-energy ion intensity depressions extended to 301/1150 UT (Figure 4b), but no ~2 MeV BIFs were detected within this ICME.

[d]Reverse shock.

[e]Details of the ICMEs and shocks at Ulysses can be found in the work of *de Koning et al.* [2005].

[f]Shock identification at Cassini based only on magnetic field data.

[g]See text for details on the ICME identification at Cassini.

[h]Shock passage at Voyager-2 occurred in a 14-hour tracking gap.

[i]Details of the MIR formation can be found in the work of *Richardson et al.* [2005].

analysis of *Skoug et al.* [2004]. Description of the energetic particle signatures observed within the ICMEs can be found in the work of *Malandraki et al.* [2005].

[13] Figures 4a and 4b show that near-relativistic electron and <1 MeV ion intensities remained above the preevent level (i.e., the instrumental background level measured on day 293) for a period of more than ~40 days. The high-energy (>40 MeV) proton intensities, however, showed only enhancements in association with the occurrence at the Sun of the most intense well-connected solar flares and fastest CMEs. Table 2 lists the solar events associated with the near-relativistic electron events shown in Figure 4a as well as the halo and partial-halo CMEs observed by the Large Angle and Spectrometric Coronagraph (LASCO) on board the Solar and Heliospheric Observatory (SOHO) during this period (CME identification and parameters were obtained from the CME catalog compiled by S. Yahiro and G. Michalek available at http://cdaw.gsfc.nasa.gov/). Association between solar flares and CMEs is based upon their temporal proximity, the site of the flare, and the direction of propagation of the CME (see also Table 1 in the work of *Dryer et al.* [2004]). The vertical arrows in Figure 4a indicate the occurrence of the events listed in Table 2. Solar events indicated in bold face in Table 2 indicate the events associated with >80 MeV proton enhancements as observed by GOES-11/EPS (Figure 4c). Ion abundances and energy spectra measured during these five SEP events are analyzed in detail in the work of *Cohen et al.* [2005]. We refer the reader to this paper for further details.

[14] The low-energy ion intensities shown in Figure 4b were measured by the Low Energy Magnetic Spectrometer LEMS120 [*Gold et al.*, 1998]. A very high fraction of the electrons that enter the LEMS120 collimator are diverted by a magnetic deflection system. However, when the >50 keV electron flux is sufficiently high, some electrons are counted in the LEMS120 ion telescope, even though the absolute efficiency for counting these electrons is quite small (~5%) [*Keeney*, 1999]. We have indicated by dotted traces the time intervals when ion channels are probably contaminated by electrons at the beginning of the large SEP events when many electrons arrive promptly, well before the slower ions start reaching the spacecraft (Figure 4b).

[15] Low-energy ion intensities peaked at or near the arrival of at least six of the CME-driven shocks observed at 1 AU (Figure 4b). The ion intensity enhancement observed on days 319–321 is classified as a CIR event due to its distinct time-intensity profile, its soft spectra, inward anisotropies (not shown here), and its association with the outward polarity high-speed solar wind stream observed on day 319 (Figure 2a). The elevated ion intensities measured during this CIR event contrast with those measured in isolated solar minimum CIR events (i.e., without the occurrence of prior intense SEP events [see, e.g., *Lario et al.*, 2001, Figure 2]). These high intensities are most likely due to reacceleration of SEPs by CIRs [*Lario et al.*, 2000b].

[16] To summarize, the successive injection of SEPs by intense solar events produced the multiple particle intensity enhancements observed at 1 AU during the time interval shown in Figure 4. The continuous acceleration of low-energy ions by CME-driven shocks and CIRs, led to the elevated low-energy ion intensities observed throughout a time period of more than 40 days (Figure 4b).

3.2. Ulysses Observations

[17] Figure 5 shows Ulysses observations in the same format as Figure 4. Figures 5a and 5b show near-relativistic electron and low-energy ion intensities measured by the HI-SCALE instrument [*Lanzerotti et al.*, 1992], whereas Figure 5c (with a different vertical scale) shows high-energy proton intensities measured by two different detectors of the COSPIN instrument [*Simpson et al.*, 1992]. The >39 MeV proton intensities were obtained from the pulse-height analysis (PHA) data of the COSPIN/HET telescope. Daily averages of the 71–94 MeV proton PHA channel are used in Figure 5c because of the limited number of PHA events

Table 2. Solar Events Associated With the Origin of the Electrons Events Observed by ACE/EPAM (Figure 3a) and Halo and Partial-Halo CMEs Observed From 19 October to 1 December 2003

	Flare				CME[a]			
Date	X Ray Onset	Class	Hα Location	NOAA AR	Time[b]	Width	V_{CME}, km s^{-1}	PA[c]
19 Oct	292/1629	X1.1/1N	N08E58	0484	292/1708	150°	472	34
21 Oct	-	-	-	-	294/0354	Halo	1484	SE+
22 Oct					295/0830	>267°	719	286
	295/0937	M1.7/	S02E22[d]	0484	295/0954	-	651[d]	255[d]
	295/1947	M9.9/	~S22E90	0486	295/2006	134°	1085	93
23 Oct	296/0817	X5.4/1B	S21E88	0486	296/0854	>236°	1406	53
24 Oct	297/0222	M7.6/1N	S19E72	0486	297/0254	123°	1055	113
	297/2135	M1.0/1N	N05W09	0484	-	-	-	-
26 Oct	299/0557	X1.2/3B	S15E44	0486	299/0654	>207°	1371	108
	299/1721	**X1.2/1N**	**N02W38**	**0484**	**299/1754**	**>171°**	**1537**	**270**
27 Oct					300/0830	144°	1322	265
28 Oct	301/0951[e]	-	-	-	301/1054	147°	1054	124
	301/1100[e]	**X17.2/4B**	**S16E08**	**0486**	**301/1130**	**Halo**	**2459**	**SE**
29 Oct	**302/2037**	**X10.0/2B**	**S15W02**	**0486**	**302/2054**	**Halo**	**2029**	**SE**
01 Nov	305/2226	M3.2/1N	S12W60	0486	305/2306	>93°	899	254
02 Nov	-	-	-	-	306/0930	Halo	2036	W+
	306/1703	**X8.3/2B**	**S14W56**	**0486**	**306/1730**	**Halo**	**2598**	**SW**
03 Nov	307/0943	X3.9/2F	N08W77	0488	307/1006	103°	1420	293
04 Nov	-	-	-	-	308/1206	Halo	1208	E+
	308/1929	**X28/3B**	**S19W83**	**0486**	**308/1954**	**Halo**	**2657**	**SW**
06 Nov	-	-	-	-	310/1730	Halo	1523	E+
07 Nov	-	-	-	-	311/1554	Halo	2237	SW+
09 Nov	-	-	-	-	313/0630	Halo	2008	SE+
11 Nov	-	-	-	-	315/0230	Halo	1359	SW+
	-	-	-	-	315/1354	Halo	1315	E+
	-	-	-	-	315/1554	128°	1785	87
12 Nov	-	-	-	-	316/1054	Halo	1197	+
13 Nov	317/0903	M1.4/	N01E90[d]	0501[d]	317/0930	>217°	1141	49
15 Nov	-	-	-	-	319/1750	148°	1375	245
17 Nov	321/0855	M4.2/1N	S01E33	0501	321/0926	>242°	1061	72
18 Nov	322/0723	M3.2/2N	N00E18	0501	322/0850	Halo	1660	SW
	-	-	-	-	322/0950	>197°	1824	95
20 Nov	324/0738	M9.6/2B	N01W08	0501	324/0806	Halo	669	SW

[a]CME classification and parameters extracted from the SOHO/LASCO CME catalog at http://cdaw.gsfc.nasa.gov/.
[b]First appearance in the C2 coronagraph (>1.5 solar radii).
[c]PA: Position Angle measured from Solar North in degrees (Counter clockwise). For halo CMEs we indicate the propagation direction of the CME (+ indicates a backside event).
[d]Based on Table 1 of *Dryer et al.* [2004].
[e]Soft X-ray emission started to increase at 301/0951 UT with an additional sharp increase at 301/1100 UT in association with the X17 flare (see Figure 2 of *Woods et al.* [2004]).

transmitted at these high energies (R. B. McKibben, private communication, 2004). Figure 5d shows magnetic field magnitude measured by the VHM on board Ulysses [*Balogh et al.*, 1992].

[18] The identification of interplanetary shocks (solid vertical lines) and ICMEs (gray vertical bars) in Figure 5 follows that given by *de Koning et al.* [2005] (see also Table 1). In Figure 5d we have identified the magnetic field enhancements associated with the passage of CIRs by the magnetic field polarity observed during the associated high-speed solar wind stream (**I** for inward and **O** for outward polarities; see Figure 2). The ICME observed by Ulysses between days 311 and 312 constitutes a specific case of an ICME interacting with a CIR [*de Koning et al.*, 2005]. The fast and wide ICME observed by Ulysses between days 320 and 324 was studied in detail in the work of *de Koning et al.* [2005]. These authors identify the solar origin of this ICME with a fast backside halo westerly directed CME observed by LASCO on day 311 (Table 2). Figure 5 shows that the passage of this ICME produced particle intensity depressions with respect to those measured at the time of the CME-driven shocks on days 317 and 319.

[19] Figure 5b shows that low-energy ion intensities were already elevated before the occurrence of the October–November 2003 events because of the effect of the recurrent CIR events observed in previous solar rotations (not shown here). Near-relativistic electron and 8–19 MeV proton intensities gradually started to increase already on day 297 (Figures 5a and 5c). We attribute these increases to the solar events occurring between days 295 and 299 on the eastern limb of the Sun (as seen from the Earth; Table 2) that slowly filled the heliosphere with energetic particles.

[20] Low-energy ion (<19 MeV) and near-relativistic electron intensities abruptly increased at 1710 UT on day 301 without any velocity dispersion effect. This increase occurred within the passage of the inward polarity CIR bounded by a forward and a reverse shock pair (Figure 5d). The X17 solar flare on day 301 (Table 2) was associated with the solar origin of the most intense SEP event observed at 1 AU [see *Cohen et al.*, 2005, Figure 4]. However, the abrupt low-energy ion (<19 MeV) intensity increase at Ulysses occurred too early to be due to injection of SEPs at the time of this flare. Our interpretation is that Ulysses suddenly established magnetic connection with a tube flux

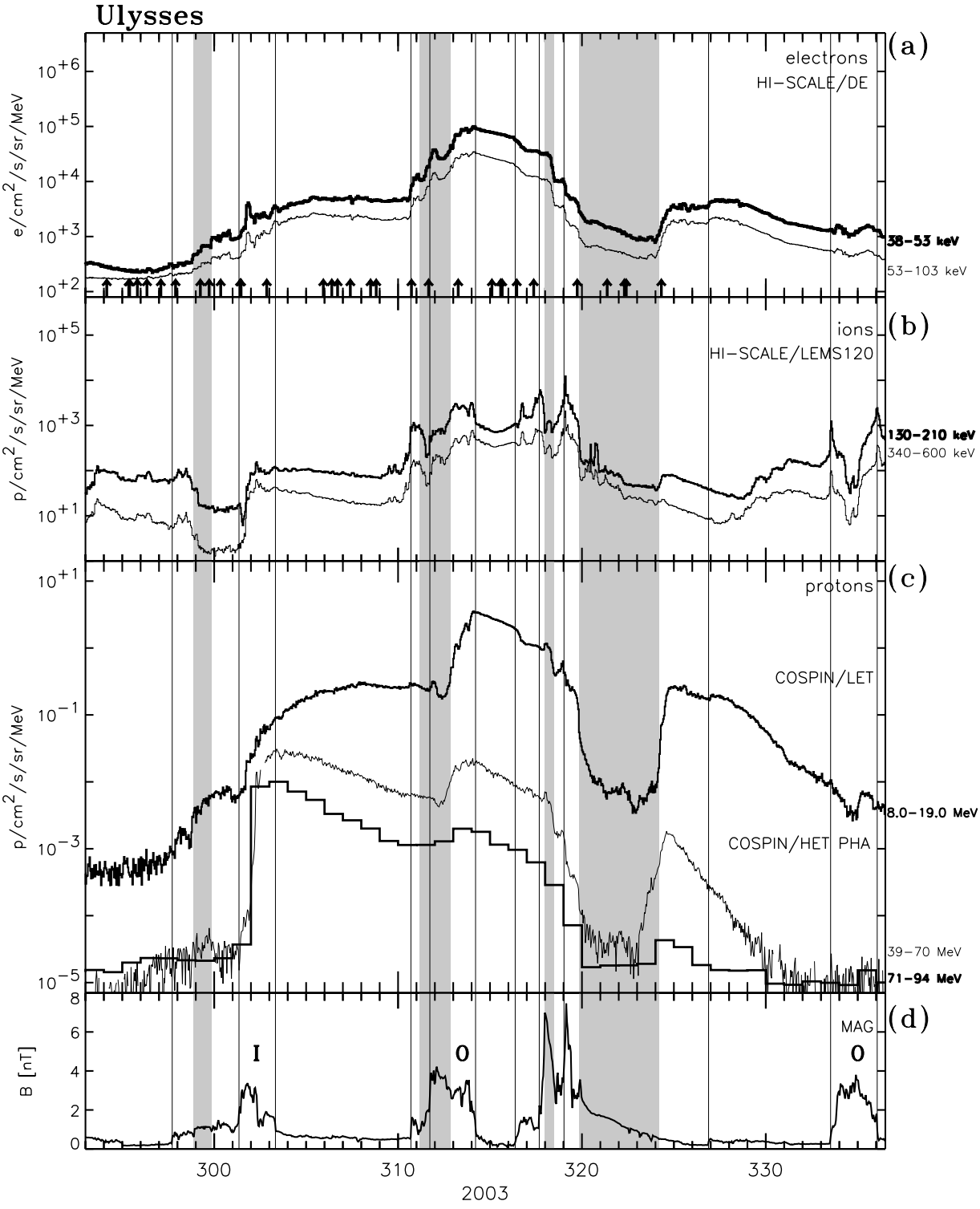

Figure 5. Spin-averaged (a) electron, (b) ion, and (c) proton intensities measured by HI-SCALE/DE [*Lanzerotti et al.*, 1992], HI-SCALE/LEMS120 [*Lanzerotti et al.*, 1992], and the COSPIN/LET and COSPIN/HET telescopes [*Simpson et al.*, 1992]. Hourly averaged intensities are shown except for the 71–94 MeV pulse-height analysis (PHA) COSPIN/HET channel where 1-day averages are shown (see details of the PHA event processing in the work of *Simpson et al.* [1992]). Vertical arrows in Figure 5a indicate the solar events listed in Table 2. (d) Hourly averages of the magnetic field magnitude as measured by VHM on board Ulysses [*Balogh et al.*, 1992]. Solid vertical lines and gray vertical bars indicate the passage of interplanetary shocks and ICMEs listed in Table 1. The heliocentric radial distance R, heliographic latitude (Λ), and inertial heliographic longitude (Ψ) of Ulysses varied from R = 5.21 AU, $\Lambda = 6.4°$, $\Psi = 79.9°$ on day 293 to R = 5.27 AU, $\Lambda = 4.1°$, $\Psi = 80.3°$ on day 336.

populated with low-energy particles that were injected into the interplanetary medium during the solar events prior to the occurrence of the X17 flare on day 301. *McKibben et al.* [2005] analyzed in detail the solar wind and magnetic field discontinuities observed within the CIR. These authors concluded that the abrupt <19 MeV ion intensity enhancement at 1710 UT on day 301 occurred in association with the passage of a stream interface formed within the CIR. According to *McKibben et al.* [2005], these energetic particles were injected from the Sun on day 299 but were not observed by Ulysses until the stream interface (that acted as a barrier for the energetic particles) reached the spacecraft. The rising intensities observed prior to the arrival of the stream interface were the result of particles that leaked through the stream interface onto field lines that intersected Ulysses (see details in the work of *McKibben et al.* [2005]).

[21] High-energy (>39 MeV) proton intensities increased at the end of day 301, about ~12 hours after the occurrence of the X17 flare on day 301. This increase was followed by a rapid enhancement at ~0545 UT on day 302. The time delay between the occurrence of the X17 flare on day 301 and these intensity increases is longer than what is expected from a zero-degree pitch-angle 70-MeV proton propagating scatter-free along a nominal Parker spiral connecting the Sun to Ulysses at 5.2 AU. Possible causes of these longer time delays include particle propagation effects over the ~13 AU field-aligned distances (assuming that the IMF topology was a undisturbed Parker spiral), delayed injection of particles onto IMF lines connecting the particle sources to Ulysses, longer path lengths than those assumed by nominal IMF topologies, and local effects by magnetic field structures crossing Ulysses that modulate the observed particle intensities (such as the inward polarity CIR observed during the onset of this event at Ulysses). The oscillations observed in the rising intensities at Ulysses were associated by *McKibben et al.* [2005] with oscillations of the magnetic field, indicating that different transport conditions existed in each flux tube.

[22] Observations at 1 AU (Figure 4) show that high-energy (>40 MeV) proton increases occurred also in association with the solar events on days 302, 306, and 308 (boldfaced in Table 2). However, no clear flux increases were observed on the already elevated intensities at Ulysses. *Lario et al.* [2000a] showed that separated SEP events at 1 AU may become merged at ~5 AU simply due to energetic particle propagation effects. Therefore it is not surprising that whereas 1 AU observations show a sequence of individual high-energy (>40 MeV) proton events (Figure 4c), Ulysses observations show only a single high-energy (>39 MeV) proton event from day 301 to 311 (Figure 5c). In addition, as observed from 1 AU, the SEP event on day 301 had a harder spectrum than the rest of SEP events shown in Figure 4c [*Cohen et al.*, 2005]. Therefore the contribution of the event on day 301 to the high-energy component of the proton intensities was larger than the subsequent events seen from 1 AU. The solar events occurring after day 301 and until day 311 injected SEPs with a softer spectrum into an already elevated particle population, resulting in an extended SEP event at Ulysses without new high-energy proton intensity enhancements (Figure 5c).

[23] The following >39 MeV proton intensity enhancement was observed by Ulysses on day 312. The most probable solar origin of this enhancement was related to the fast backside halo CMEs on days 310 and 311 (Table 2). The easterly directed backside halo CME on day 310 did not produce any effect on the already decaying intensities at 1 AU (Figure 4), whereas the event on day 311 produced only a small near-relativistic electron event at 1 AU (Figure 4a). The onset of this event at Ulysses was modulated by the passage of an ICME and an outward polarity CIR on days 311–313 (Figure 5d). Details of the high-energy component of this particle intensity enhancement can be found in the work of *McKibben et al.* [2005].

[24] An additional high-energy proton intensity increase was observed by Ulysses on day 323 near the passage of the trailing edge of the fast ICME. Analysis of the ion anisotropy flows allows us to discern whether this new particle intensity enhancement was due to either a recovery of particle intensities after the passage of the ICME or a new injection of SEPs from the Sun. Figure 6 shows the evolution of the 1.87–4.80 MeV ion anisotropy coefficients measured in the solar wind frame from day 298 to 338 as observed by the Ulysses/HI-SCALE instrument [*Lanzerotti et al.*, 1992]. These coefficients are deduced from the sectored data collected by the LEMS30 and LEMS120 telescopes, transformed into the solar wind frame by correcting for the Compton-Getting effect, and fitting a reduced second-order spherical harmonic expansion (see *Sanderson et al.* [1985] for details). The first-order harmonic consists of three components with amplitudes A_1, A_{11}, and B_{11}. The ratio A_1/A_0 (where A_0 is the isotropic component; Figure 6a) represents, in the solar wind frame, the first-order anisotropy resolved along the magnetic field direction (its sign is defined with respect to the IMF direction). A_{11} and B_{11} represent the flow transverse to the IMF and are practically zero throughout the time interval covered in Figure 6, indicating that there was no net flow of particles across the IMF (Figures 6c and 6d). Finally, the quantity A_2/A_0 (Figure 6e) represents the second-order harmonic distribution. A positive ratio of A_2/A_0, when the first-order coefficients are close to zero, represents a bidirectional ion flow (BIF) along the IMF [*Sanderson et al.*, 1985]. Details about the computation of the anisotropy coefficients can be found in the work of *Lario et al.* [2004b].

[25] In Figure 6b we have identified the periods when the particle flows were directly outward along the IMF (indicated by plus symbol), inward along the IMF (indicated by minus symbol), and when BIFs were observed (indicated by **B**). The particle intensity enhancements on days 301, 313, and 324 showed outward flows along the field, whereas the shocks on days 310, 311, 319, and 336 produced changes in the particle flows indicating that these low-energy ions were flowing away from the shocks and hence most likely locally accelerated by the shocks.

[26] The passage of the fast ICME by Ulysses during days 320–324 was characterized by particle intensity depressions (Figure 5) and ~2 MeV BIFs (Figure 6). Both signatures are typical of the passage of ICMEs at 1 AU [*Richardson*, 1997]. In this case, they were also observed at 5.2 AU. The outward particle flow observed after the passage of the ICME suggests that the new intensity

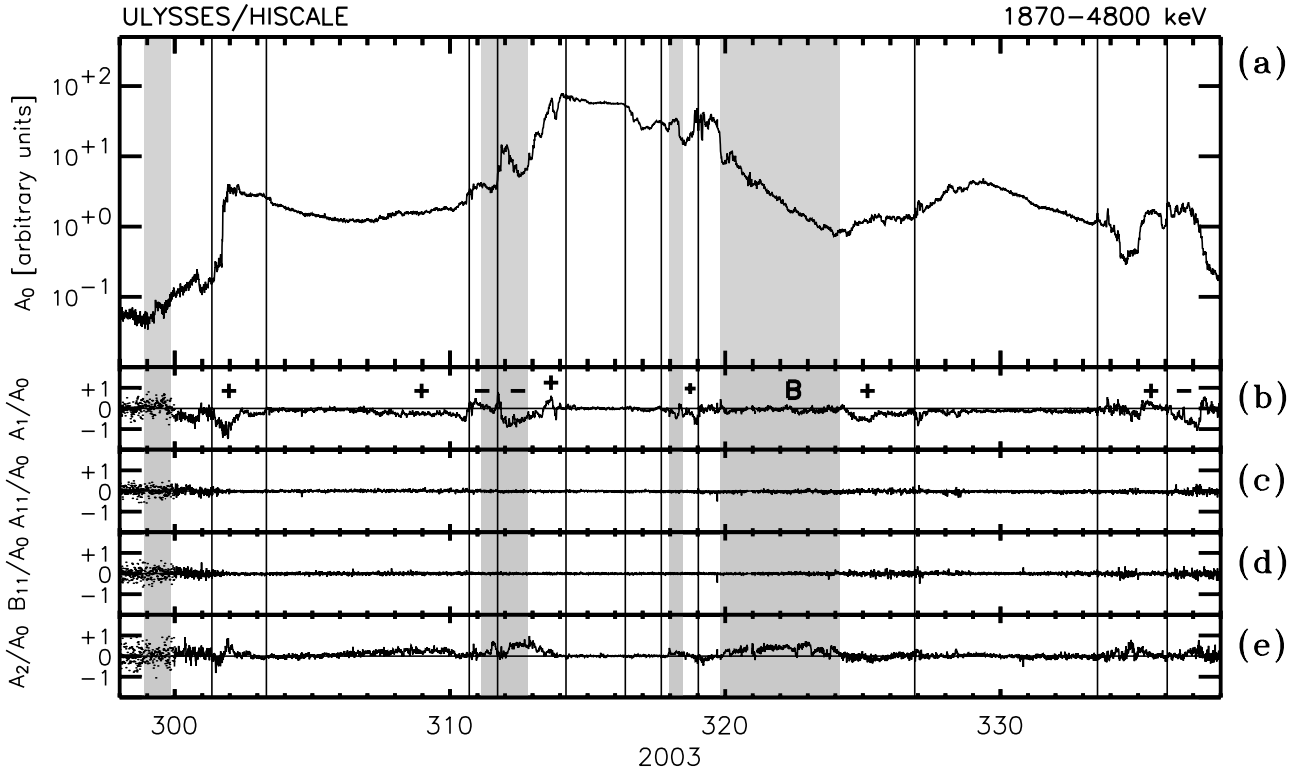

Figure 6. Anisotropy flow coefficients in the solar wind frame as inferred from the LEMS30 and LEMS120 telescope measurements of the HI-SCALE instrument on board Ulysses [*Lanzerotti et al.*, 1992]. Solid vertical lines and gray vertical bars indicate the passage of interplanetary shocks and ICMEs listed in Table 1. The plus and minus symbols in Figure 6b identify the antisunward and sunward flow directions, respectively, whereas the period inside the fast ICME (indicated by **B**) was characterized by BIFs.

enhancement on day 324 was due to an injection of SEPs from the Sun (probably associated with the fast halo CMEs on day 322; Table 2) and not to a recovery of the fluxes observed prior to the ICME passage. Note also that the 8–19 and 39–70 MeV peak intensities at the end of day 324 were higher than what is expected following the decay trend established before the passage of the ICME (Figure 5c). The energy spectra of this new particle injection was softer than the previous high-energy proton intensity enhancements seen by Ulysses. The arrival of these freshly injected particles was mediated by the passage of the ICME. Low-energy ions and near-relativistic electrons were only observed once the ICME was beyond Ulysses, whereas the >39 MeV protons were able to propagate across or within the ICME as observed in the already increasing 39–70 MeV proton flux on day 323 (Figure 5c). The low count rates of the 71–94 MeV proton channel forced us to use 1-day averages in Figure 5c and we cannot discern whether the new injected >70 MeV propagated inside the ICME. The access of energetic particles into the ICME depends upon both the magnetic topology of the ICME and the energy, gyroradii, and source of the energetic particles [*Lario et al.*, 2004b]. This discussion is beyond the scope of the present study. In any case, Figure 5 shows that the intensity increase was more pronounced after the trailing edge of the ICME moved past Ulysses, suggesting that the transport of particles to Ulysses was impeded by this intervening structure.

[27] To summarize, Ulysses observations show that, as in the case of 1 AU observations (Figure 4), near-relativistic electron and <1 MeV ion intensities remained high (i.e., above the preevent level measured on day 299 for ions and on day 296 for electrons) for a long (>40 days) period of time. For example, the 340–600 keV ion intensity did not come back to the values measured on day 299 until day 345. These high intensities resulted from both the injection of SEPs from the Sun during the October–November 2003 events, and the effects that both CME-driven shocks and recurrent CIRs have in the interplanetary medium being able to reaccelerate low-energy particles.

3.3. Cassini Observations

[28] Figure 7 shows energetic particle and magnetic field observations from the Cassini spacecraft. Energetic particle data were collected by the Low-Energy Magnetospheric Measurement System (LEMMS) of the Magnetospheric Imagining Instrument (MIMI) [*Krimigis et al.*, 2004], whereas the magnetic field data comes from the VHM on board the Cassini spacecraft [*Dougherty et al.*, 2004]. Unfortunately, the plasma instrument on Cassini was not orientated to observe the solar wind flow; therefore we use magnetic field data to determine the passage of shocks. The use of magnetic field data alone to identify plasma structures prevents us from performing their complete characterization and classification. In Figure 7d we have identified

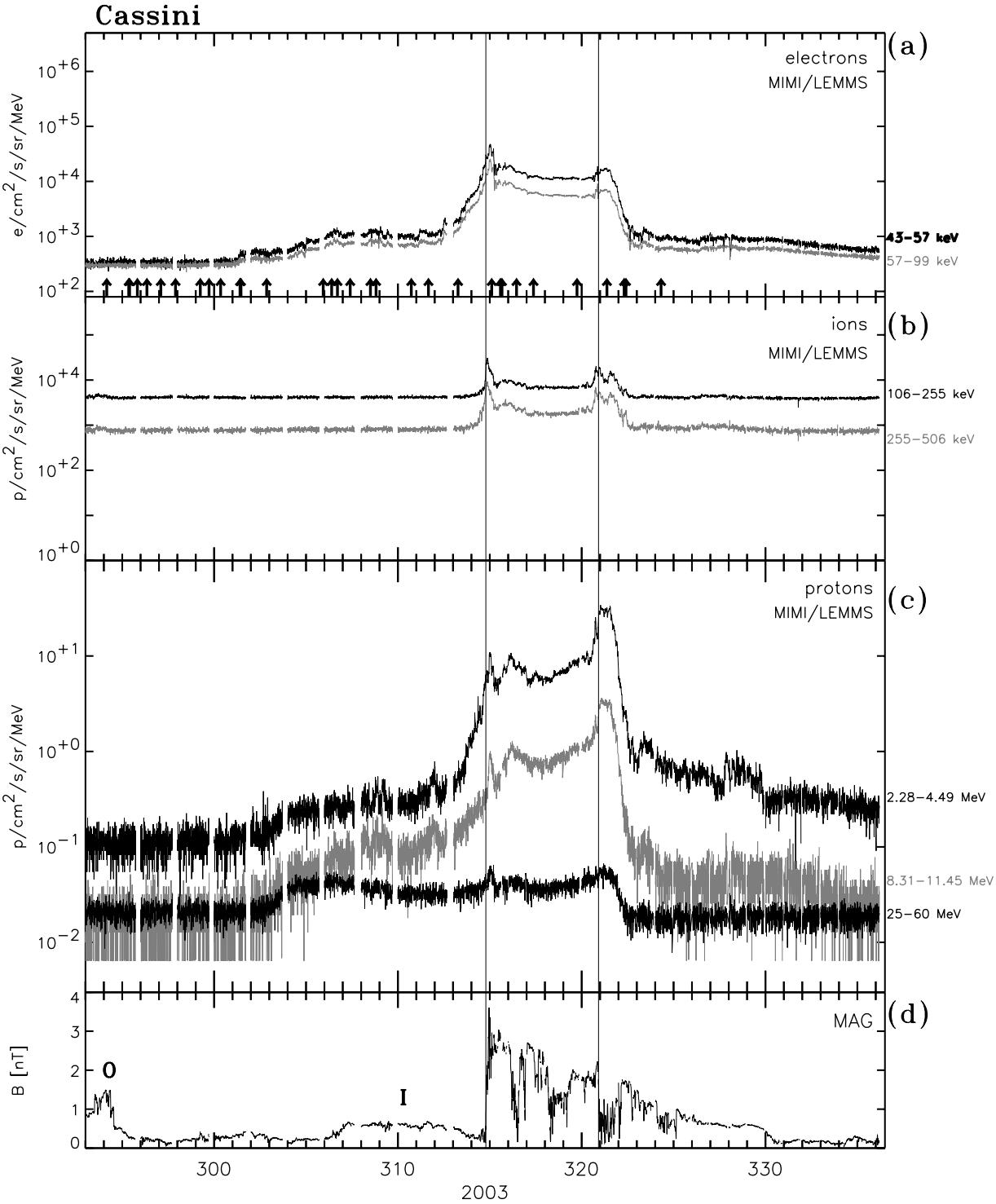

Figure 7. Ten-minute averages of the (a) electron, (b) ion, and (c) proton intensities measured by MIMI/LEMMS on board Cassini [*Krimigis et al.*, 2004]. Vertical arrows in Figure 7a indicate the solar events listed in Table 2. (d) Hourly averages of the magnetic field magnitude as measured by VHM on board Cassini [*Dougherty et al.*, 2004]. Solid vertical lines indicate the passage of possible interplanetary shocks listed in Table 1. The heliocentric radial distance R, heliographic latitude (Λ) and inertial heliographic longitude (Ψ) of Cassini varied from R = 8.65 AU, $\Lambda = -3.5°$, $\Psi = 25.5°$ on day 293 to R = 8.73 AU, $\Lambda = -3.6°$, $\Psi = 26.4°$ on day 336.

two magnetic field discontinuities (solid vertical lines) that are presumably a forward and a reverse shock (their arrival times are listed in Table 1) bounding a structure with enhanced highly fluctuating magnetic field (see also Figure 2c).

[29] The solar origin of this enhanced magnetic field structure is uncertain because of the intense level of solar activity occurring during this time interval (Table 2). Besides, this structure moved past Cassini when an outward polarity CIR structure was expected to be observed (Figure 2c). The interaction between solar wind streams results in regions of enhanced magnetic field magnitude [*Burlaga and Ogilvie*, 1970]. We suggest that the interaction and coalescence of the numerous CMEs occurring at that time (mostly westerly directed, see Table 2), together with the outward polarity CIR, formed this enhanced magnetic field structure. *Richardson et al.* [2005] used a one-dimensional MHD model to propagate radially outward the plasma structures observed at 1 AU during this time interval (Figures 2a and 4d). At a distance of 8.7 AU, they obtained a forward shock in the middle of day 315 associated with the shock observed by ACE at 0558 UT on day 302. According to their model, the shock at 8.7 AU was followed by a low-density region from the middle of day 318 to late on day 323 when a new forward shock, related to the shock seen by ACE at 1619 UT on day 303, arrived at 8.7 AU. Differences between the structures obtained by *Richardson et al.* [2005] at 8.7 AU and the Cassini observations could be due to the longitudinal separation between ACE and Cassini as well as the multiple CMEs expanding outward from various longitudes (Table 2).

[30] The enhanced magnetic field structure observed by Cassini (Figure 7d) lasted ~15 days (from late on day 314 until day 330). The field direction varied considerably from day 316 to day 325 whereas from day 325 to 330 a period with low-variance in both magnetic field magnitude and components was observed (Figure 2c). Detailed analysis of the individual features present within this large-scale structure and their identification with specific solar events are beyond the scope of this paper. The long duration of this event, the enhanced level of fluctuations in the magnetic field directions, together with the occurrence of multiple CMEs at the Sun, suggest that this field structure was part of a compound stream as defined by *Burlaga* [1975]. Similar examples of formation of compound streams are described elsewhere [e.g., *Burlaga et al.*, 1986].

[31] Particle intensities measured by the MIMI/LEMMS are affected by high background rates mostly due to the Radioisotope Thermoelectric Generator (RTG) and the galactic cosmic ray background [*Lario et al.*, 2004a]. Figures 7a, 7b, and 7c show electron, ion, and proton intensities without any background subtraction. Enhanced low-energy ion intensities (Figure 7b) were only observed during the passage of the enhanced magnetic field structure, whereas the rest of the period plotted in Figure 7b only shows intensities at background level.

[32] Electron intensities (Figure 7a) started to gradually increase above the background at the beginning of day 301. This increase was followed by a new gradual enhancement at the end of day 302 that continued until day 313 when intensities rose by more than one order of magnitude and peaked after the passage of the forward shock on day 314. High electron intensities were observed between the passage of the two shocks and abruptly decreased on day 322. The 25–60 MeV proton intensities (Figure 7c) started to gradually increase above the background at the end of day 302 reaching a first maximum on day 306 followed by a slow gradual decay of more than 8 days. The 25–60 MeV proton intensities peaked after the passage of the two shocks, remaining high between the two shocks and rapidly decreasing on day 322.

[33] As in the case of Ulysses, we attribute the first electron intensity increase (at the beginning of day 301) to the solar events occurring prior to day 301, whereas the subsequent increase seen in both the 25–60 MeV proton and near-relativistic electron channels at the end of day 302 was mainly a result of the particle injection during the main solar event on day 301. The merging of SEP events at larger heliocentric distances [*Lario et al.*, 2000a], the softer spectrum of the new solar events at 1 AU (Figure 4c), the deceleration of energetic particles propagating to Cassini, and the mitigating effect that intervening transient solar wind flows have on the prompt component of the SEP events [*Lario et al.*, 2004a] are the possible reasons that no additional increases in the Cassini particle intensities were observed in association with the solar events occurring after day 302.

[34] *Lario et al.* [2004a] showed that during the heliospheric cruise of Cassini to Saturn (at heliocentric radial distances ranging between 2.5 and 8.0 AU) the arrival of SEPs at Cassini was modulated by the presence of magnetic field structures formed between the Sun and Cassini. The structure of the inner heliosphere prior to the occurrence of the October–November 2003 events was dominated by the two recurrent high-speed streams (Figure 3). However, the series of solar events started with the appearance of the active regions AR0484 and AR0486 already on the eastern limb of the Sun (Table 2), producing a series of transient flows propagating toward these longitudes [*Dryer et al.*, 2004]. The presence of such a system of transient flows in the field lines connecting Cassini to the Sun may have had a mitigating effect on the prompt component of the SEP events [*Lario et al.*, 2004a]. Comparison with the other SEP events observed during the Cassini heliospheric cruise (Figure 1 in the work of *Lario et al.* [2004a]) shows that the prompt component of the October–November 2003 SEP events at Cassini (i.e., the intensity enhancement observed from day 302 to day 312) was not intense. This result can be explained in terms of both the modulating effect of the intervening structures propagating between the Sun and Cassini and the larger heliocentric radial distance of Cassini [*Lario et al.*, 2004a].

[35] The time histories of the October–November 2003 events at Cassini were completely controlled by the passage of the enhanced magnetic field structure. The proton intensities above 2.2 MeV (Figure 7c) peaked on day 321 just after the shock passage on day 320 and coinciding with a depression of the magnetic field magnitude (Figure 7d). The abrupt decrease in particle intensities observed on day 322 and the increase in magnetic field magnitude suggests that Cassini entered into a new structure of this large-scale compound stream. Therefore particle intensities were modulated by the passage of local magnetic field structures. Unfortunately, the LEMMS experiment was looking to a

fixed direction in the sky during most part of the time interval considered in Figure 7. Consequently, we have not computed particle anisotropies for Cassini and the analysis of the effect that these local structures had on the flow of energetic particles is not available.

3.4. Voyager-2 Observations

[36] Unlike the other spacecraft used in this analysis, Voyager-2 was located in the outer heliosphere (R = 71.6 AU) and south of the ecliptic plane ($\Lambda = -24.8^\circ$) at the time of the October–November 2003 solar events (Figure 1). The system of transient flows generated during this series of events was predicted to arrive at Voyager-2 around day 119 of 2004, when Voyager-2 was at R = 73.18 AU, $\Lambda = -25.2^\circ$, and $\Psi = 215.3^\circ$ [*Richardson et al.*, 2005]. Figure 8 shows energetic particle data from the Low Energy Charged Particle (LECP) experiment [*Krimigis et al.*, 1977] and solar wind speed from the Plasma Science (PLS) experiment [*Bridge et al.*, 1977] on board Voyager-2. The solid vertical line in Figure 8 identifies the passage of a shock (Table 2) driven by the merged interaction region (MIR) formed as a result of the series of events in October–November 2003 [*Richardson et al.*, 2005; *Burlaga et al.*, 2005a]. The averaged transit speed of this MIR to travel from the Sun to Voyager-2 was about ~690 km s^{-1}. Voyager-2 solar wind observations prior to the occurrence of these events were described by *Burlaga et al.* [2005b]. The recurrent CIRs observed at 1–9 AU prior to the October–November 2003 events (Figure 2) were not observed by Voyager-2 because they were overtaken by the faster CMEs ejected from the Sun. However, the period prior to the arrival of the MIR at Voyager-2 was characterized by an increase of the solar wind speed due to the reappearance of coronal holes at the Sun [*Burlaga et al.*, 2005b].

[37] Magnetic field data from Voyager-2 were analyzed in the work of *Burlaga et al.* [2005a]. Within the ~48 days time period with elevated solar wind speeds, i.e., from the shock passage on day 119 until day ~167 (Figure 8d), *Burlaga et al.* [2005a] identified the following magnetic structures: the shock (on day 119), a sheath-like region (from the shock up to day 128), and a relatively fast stream with smooth speed profile that decreased monotonically until at least day 167 (see Figure 2 in the work of *Burlaga et al.* [2005a]).

[38] Figures 8a, 8b, and 8c show the energetic particle intensities measured by Voyager-2 during this event. Intensities of the LECP energy channels were corrected for background by subtracting counts due to penetrating cosmic rays. The 3.0–17.3 MeV proton intensities began rising ~25 days prior to the passage of the shock, peaked ~1 day after the shock arrival and remained elevated for a period of ~70 days (Figure 8c). The 22–30 MeV proton channel (not shown here) did not show any intensity enhancement during this period, whereas the cosmic-ray dominated >70 MeV proton intensities (not shown here) showed an ~8% decrease with respect to the intensities measured at the time of the shock passage. The >70 MeV proton intensity depression began on day 128 (9 days after the shock passage) in association with an increase in magnetic field magnitude [*Burlaga et al.*, 2005a]. The minimum of the >70 MeV proton intensity was reached on day 138 (19 days after the shock) coincident with the maximum of the magnetic field magnitude. The reader is referred to the work of *Burlaga et al.* [2005a] for further details on the evolution of the cosmic ray intensities during this event.

[39] Figure 8b shows that the low-energy (<200 keV) ion intensities began rising just a few (~10) days before the shock passage and peaked ~15 days after the shock. The intermediate-energy (540–3500 keV) ion intensities showed two peaks ~4 days and ~16 days after the shock, whereas the 3.0–17.3 MeV proton intensities (Figure 8c) peaked ~1 day after the shock. While the >3 MeV proton time-intensity histories were dominated by the first peak close to the shock passage, the <200 keV ion time-intensity histories were dominated by the second peak observed a few (10–15) days after the shock and contained in the region of enhanced magnetic field [*Burlaga et al.*, 2005a]. The electron intensity profiles (Figure 8a) resemble those of the 3.0–17.3 MeV protons, rising ~15 days before the shock passage and peaking ~5 days after the shock. Electron intensity enhancements were also observed at the highest-energy electron channel of the LECP instrument (0.35–1.50 MeV).

[40] In contrast to the observations in the inner heliosphere, the particle event at Voyager-2 was only observed at energies below 17 MeV and in association with the passage of the MIR. The duration of the time interval with enhanced proton intensities increased with the proton energy. Since low-energy ion intensities did not peak at the time of the shock passage, we suggest that the shock did not locally accelerate particles. The fact that low-energy (<200 keV) ion intensities peaked ~15–20 days after the shock passage suggests that these particles were part of a particle population accelerated earlier in the event either during the solar events or by the traveling shocks when they were still close to the Sun and efficient enough to accelerate particles. These low-energy particles propagated along the highly twisted IMF in the outer heliosphere, undergoing adiabatic deceleration. The expanding MIR and associated shock were able to overtake these particles that remained confined behind the shock by the magnetic structures formed in the MIR (similar examples have also been suggested by *Decker and Krimigis* [2003]). Energetic particles observed before and during the shock arrival may consist of an ambient population that was magnetically reflected and swept ahead by the MIR bearing an enhanced magnetic field [*Decker and Krimigis*, 2003].

4. Discussion

[41] The series of solar events occurring in October–November 2003 produced SEP events with diverse time-intensity histories at the different spacecraft where they were observed. At 1 AU multiple intensity enhancements were observed in association with the intense solar events occurring at the Sun. Whereas low-energy ion intensities peaked at the time of the shocks, the high-energy particle enhancements were due to the fresh injection of SEPs from the Sun (Figure 4). At 5.2 AU, particle intensities were modulated by the passage of a fast ICME and the effects of the CIRs (Figure 5). Ulysses high-energy proton intensities showed only three gradual enhancements that contrasted with the multiple injections observed at 1 AU. At 8.7 AU

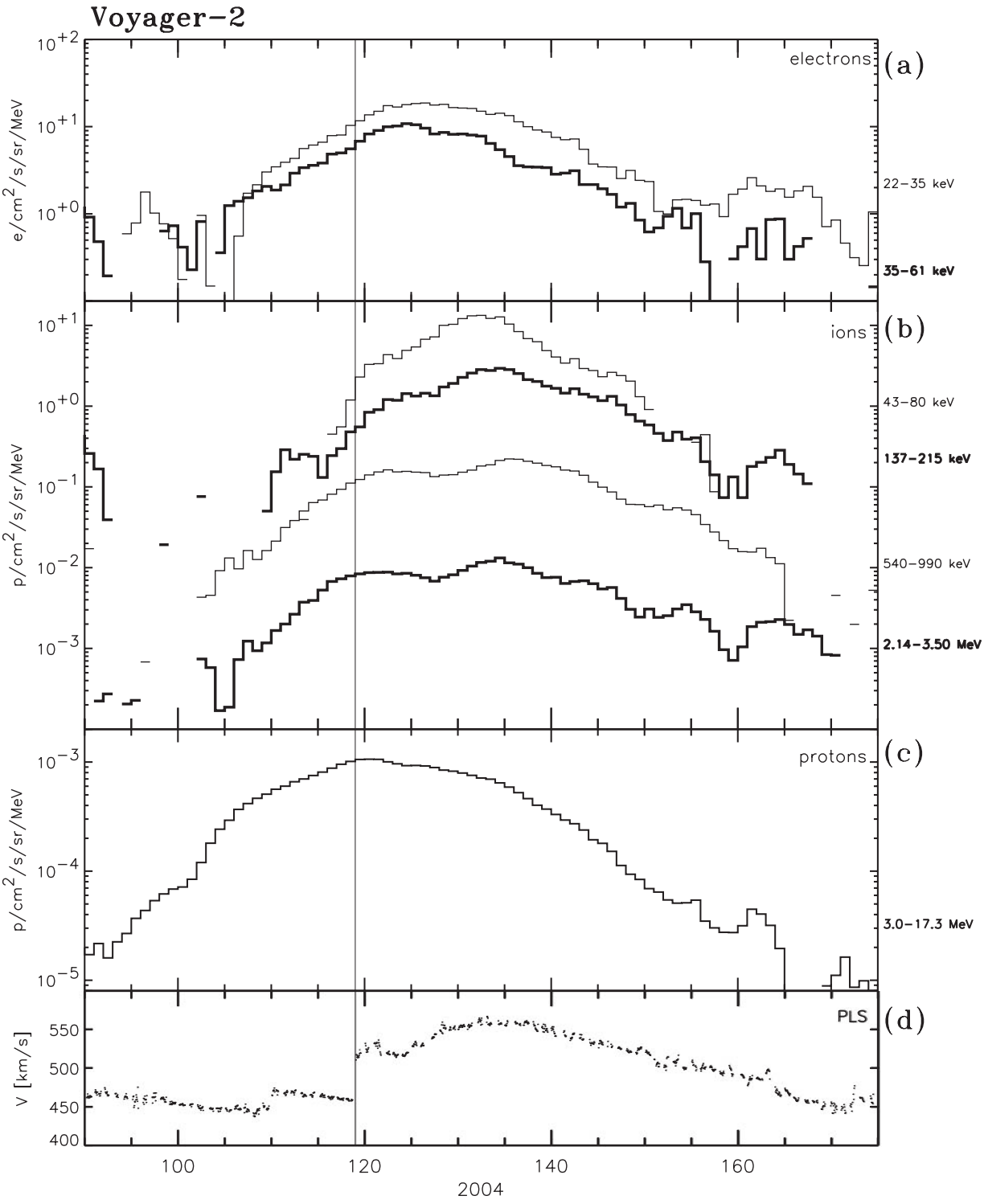

Figure 8. Five-day running averages of 1-day averages of the (a) electron, (b) ion, and (c) proton intensities measured by LECP on board Voyager-2 [*Krimigis et al.*, 1977]. (d) Hourly averages of the solar wind speed as measured by PLS on board Voyager-2 [*Bridge et al.*, 1977]. Solid vertical line indicates the passage of an interplanetary shock as listed in Table 1. The heliocentric radial distance R, heliographic latitude (Λ) and inertial heliographic longitude (Ψ) of Voyager-2 varied from R = 72.93 AU, $\Lambda = -25.1°$, $\Psi = 215.3°$ on day 90 to R = 73.66 AU, $\Lambda = -25.3°$, $\Psi = 215.4°$ on day 175.

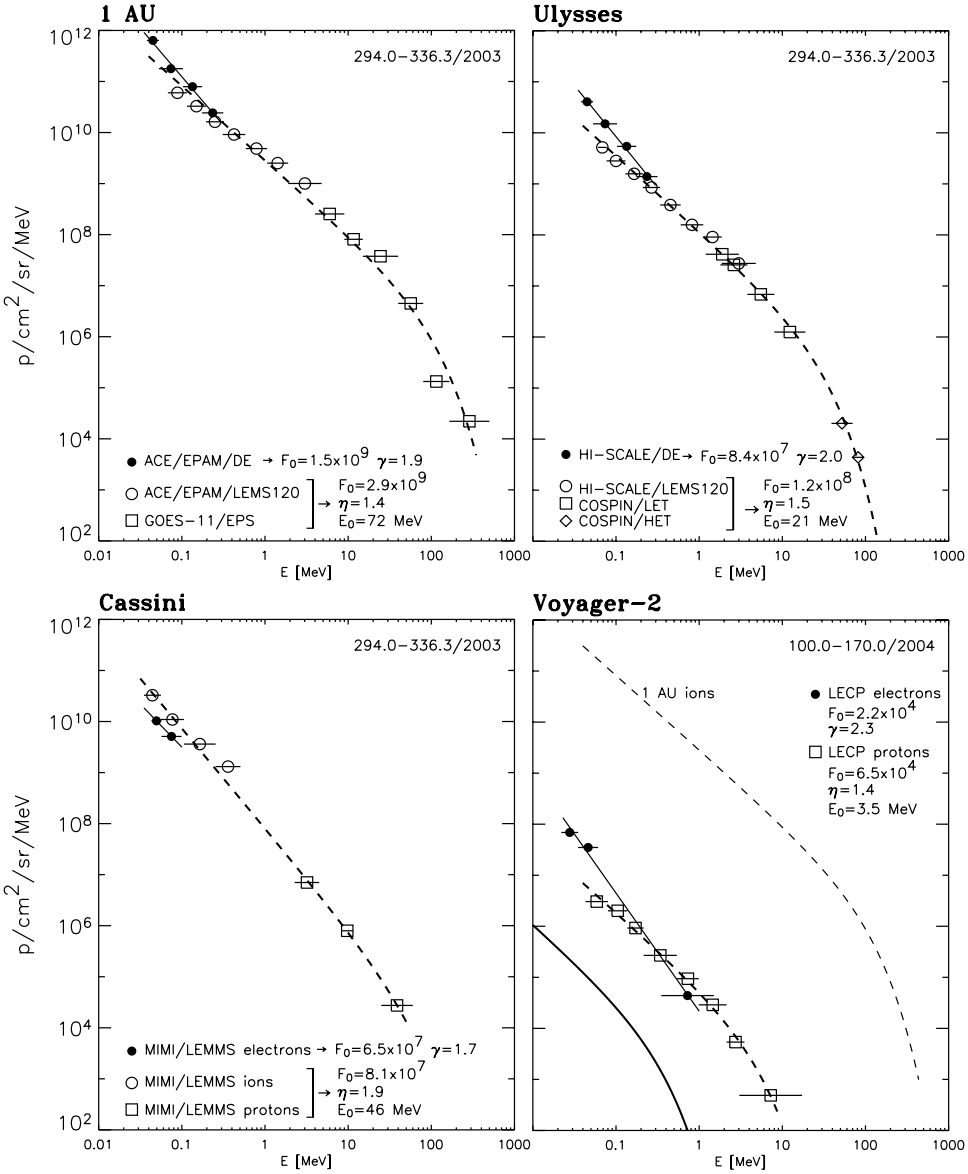

Figure 9. Energy spectra of the particle fluence measured at the four different heliospheric locations. Solid and dashed lines are the result of fitting $F = F_0E^{-\gamma}$ to the fluence inferred from the electron channels (solid symbols) and $F = F_0E^{-\eta}\exp(-E/E_0)$ to the fluence inferred from the combination of ion and proton channels (open symbols), respectively. Subtraction of the preevent intensities from the Cassini fluxes removes most of the contribution of RTG and cosmic rays counts into the fluences shown in the lower left panel. The lower right panel also shows the ion fluences measured at 1 AU (thin dashed line) and those predicted by assuming adiabatic cooling expansion (thick solid line).

the time-history enhancements were observed in association with the passage of an enhanced magnetic field structure, whereas the prompt component of the SEP event associated with the X17 flare on day 301 was largely reduced (Figure 7). Finally, at 73.1 AU, only a <20 MeV proton intensity enhancement was observed in association with the passage of a MIR (Figure 8).

[42] The diversity of the time-intensity histories observed at the different spacecraft was due to both the multiple particle injections occurring at different times and longitudes (Table 2) and the passage over the spacecraft of magnetic structures controlling the particle intensities. The common feature of the events at all radial distances was the long time interval with elevated particle intensities. In the following, we study the evolution of the particle fluence integrated over the duration of the events at each spacecraft and the possible formation of energetic particle reservoirs in the inner heliosphere.

4.1. Energetic Particle Fluences

[43] Figure 9 shows the energy spectra of the particle fluence evaluated over the time interval shown in Figures 4, 5, and 7 for 1 AU, Ulysses, and Cassini, and from day 100 to 170 of 2004 for Voyager-2. To compute the fluence F (in

units of particles cm^{-2} sr^{-1} MeV^{-1}), we have first subtracted the preexisting intensity observed before the onset of the particle enhancement and then integrated the differential fluxes measured in each energy channel over the above indicated time interval. The preevent flux subtraction takes care of most of the RTG and galactic cosmic ray background contributions to the particle intensities measured by Cassini, since presumably both sources were relatively constant during the time interval shown in Figure 7. We suspect that the actual fluences of the October–November 2003 events at 8.7 AU were not higher than the fluences deduced using Cassini measurements and shown in the lower left of Figure 9.

[44] We have fitted a power law $F = F_0E^{-\gamma}$ to the fluence inferred from the electron channels and an exponential rollover function $F = F_0E^{-\eta}\exp(-E/E_0)$ to the combination of ion and proton channels (in the above equations, E units are MeV and F_0 units are cm^{-2} sr^{-1} MeV^{-1}). The values of the fitting parameters are given in each panel of Figure 9. Assuming a correct intercalibration between the different instruments on board each spacecraft, we obtain a radial dependence for F_0 as $R^{-2.6}$ and $R^{-2.5}$ for electrons and protons, respectively.

[45] It is of interest to compare the ion fluence spectrum observed at Voyager-2 with that expected if the fluence spectrum at 1 AU were simply convected to the Voyager-2 helioradius. This is a good approximation since convection effects are expected to dominate the propagation of low-energy ions in the outer heliosphere. Taking the midpoint times of the Voyager-2 and 1-AU averaging intervals as reference times and assuming spherically symmetric expansion, the ion distribution observed at 1 AU on day 315 of 2003 reached Voyager-2 (at 73.3 AU) on day 135 of 2004, implying a mean propagation speed of ~680 km s^{-1} during the 185 day transit from 1 to 73.3 AU. Let us assume that during this half-year interval, a "shell" of ions was isotropically locked into the plasma and underwent adiabatic cooling during its convection to Voyager-2. Then, the particle distribution function $f(r, p)$ at radius r and momentum p would satisfy $V\frac{\partial f}{\partial r} = \frac{1}{3}\frac{2V}{r}p\frac{\partial f}{\partial p}$ [*Skilling*, 1975; equation (15)], where V is the solar wind speed. Thus $f(r, p)$ is constant along characteristics curves $rp^{3/2} = const$ in the $r - p$ plane, i.e., $f(r, p) = f_0(r_0, p_0)$ for $rp^{3/2} = r_0p_0^{3/2}$. The differential intensity $j(r, T) = p^2f(r, p)$ is related to the differential intensity $j_0(r_0, T_0)$ measured at r_0 and kinetic energy $T_0 = \frac{p_0^2}{2m}$ by

$$j(r,T) = \left(\frac{p}{p_0}\right)^2 j_0(r_0,T_0) = \left(\frac{r_0}{r}\right)^{4/3} j_0\left(r_0, T_0 = T(r/r_0)^{4/3}\right). \quad (1)$$

This expression allows us to calculate $j(r, T)$ at Voyager-2 (r = 73.3 AU) at the measured energy T given $j_0(r_0, T_0)$ at r_0 = 1 AU evaluated at $T_0 = T(\frac{r}{r_0})^{4/3}$. The lower right of Figure 9 shows the ion fluences predicted at 73.3 AU (thick solid line) using both equation (1) and the fluences measured at 1 AU (thin dashed line). The larger fluences measured by Voyager-2 during the October–November 2003 events suggests that processes not included in this simple model such as particle reacceleration by propagating shocks (as observed at Ulysses) and/or additional particle sources contributed to the event observed at Voyager-2.

[46] Figure 9 also shows that whereas electron fluences are above the ion fluences at 1 and 5.2 AU, Cassini observed lower electron fluences. A possible interpretation is that at this distance, particle intensities were observed exclusively in association with the passage of two shocks and that ion shock acceleration in the interplanetary medium is more efficient than electron acceleration. On the other hand, the <61 keV electron fluences at Voyager-2 were above those measured for the ions, suggesting the contribution of an additional electron population associated with, for example, cosmic ray electrons swept by the MIR and observed before the arrival of the shock (see discussion in the work of *Decker and Krimigis* [2003]).

4.2. Energetic Particle Reservoirs

[47] Multispacecraft observations of energetic particle intensities have shown that particle fluxes measured during the decay phase of large SEP events often present equal intensities that evolve similarly with time [*McKibben*, 1972]. These periods of small longitudinal, latitudinal, and radial particle intensity gradients, named reservoirs by *Roelof et al.* [1992], have been observed during isolated major SEP events [*McKibben et al.*, 2003; *Lario et al.*, 2003] and during periods of intense solar activity when a sequence of events occurred at the Sun [*Roelof et al.*, 1992; *Maclennan et al.*, 2001]. Possible mechanisms for the formation of particle reservoirs are described in the work of *Lario et al.* [2003]. The October–November 2003 series of events with elevated intensities for long time intervals seems appropriate for the formation of a particle reservoir.

[48] Figure 10 shows ~40 keV electron intensities measured by ACE, Ulysses, and Cassini from day 294 to 336. With the exception of a ~2 day interval from day 322 to 324, when Ulysses and Cassini observed simultaneously similar electron intensities, no other period with equal electron intensity was simultaneously observed. During this 2-day interval (322–323), Ulysses was within the fast ICME (Figure 5) and Cassini was still immersed in the compound stream that moved past this spacecraft (Figure 7). Electron intensities during this period, however, were already depressed due to the passage of these plasma structures over the two spacecraft.

[49] Figure 10 shows multiple electron intensity enhancements at ACE from day 294 to 311 that contrast with the gradual enhancement observed by Ulysses from day 297 to 311. Figure 9 of *Lario et al.* [2000a] shows that multiple solar injections separated by a short time interval may be observed at 1 AU as distinct SEP events but as a single smooth profile at 5 AU simply due to propagation effects.

[50] The highest electron intensities at Ulysses were observed between days 314 and 316, just after the passage of the CIR structure on day 313 and before the arrival of the forward shock on day 316 (Table 1). During this time interval, ~2 MeV ion anisotropy coefficients were remarkably close to zero (Figure 6), consistent with a particle population stagnated between these two structures and convected with the solar wind speed. Similar periods of isotropic enhanced particle intensities at Ulysses confined

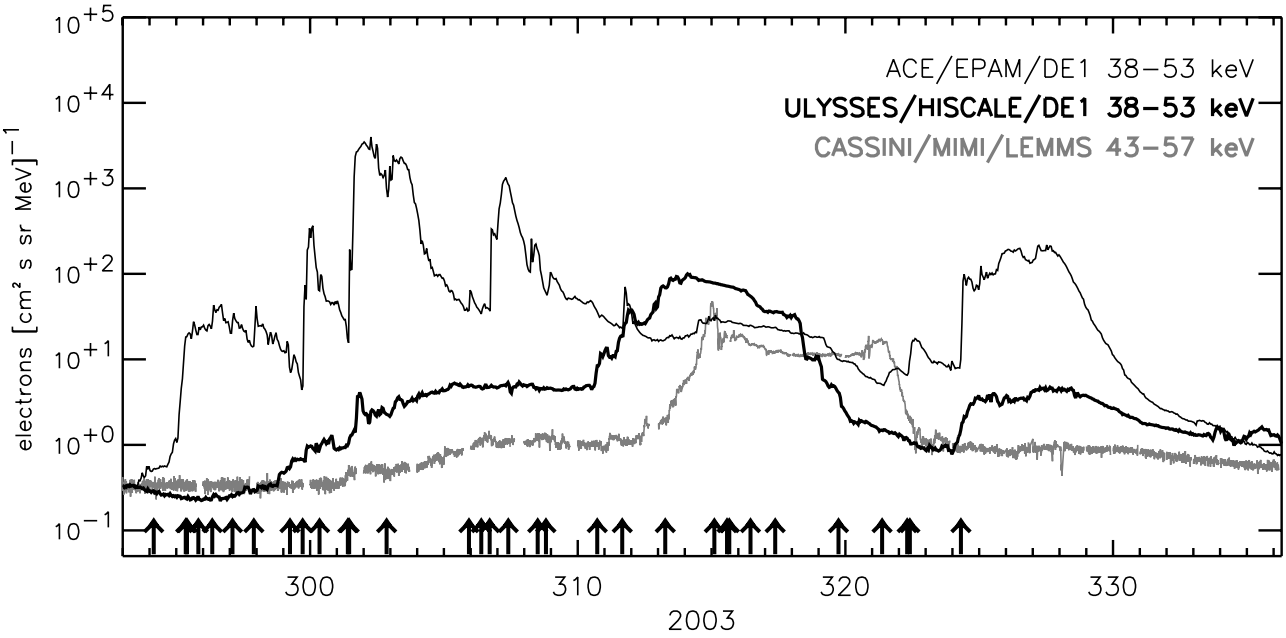

Figure 10. Electron intensities measured in similar energy channels by ACE, Ulysses and Cassini from day 293 to 336. Vertical arrows indicate the occurrence of the solar events listed in Table 2.

between two enhanced magnetic field structures have been previously observed by Ulysses (e.g., when it was at 5.2 AU in November 1998; see Figure 8b of *Lario et al.* [2000a]).

[51] The highest electron intensities at Cassini were observed during a period of ~8 days (314–321) also in association with the passage of the enhanced transient magnetic field structure (Figure 7). *Kallenrode and Cliver* [2001] suggested that the presence of two converging shocks is an appropriate situation to generate long-lasting periods of high ion intensities. The proposed mechanisms leading to these high ion intensities are the formation of strong magnetic field enhancements that act as both ion reaccelerators and as efficient barriers for particle mirroring [*Kallenrode and Cliver*, 2001]. Reflection of near-relativistic electrons by enhanced magnetic field structures and electron acceleration by traveling interplanetary shocks at distances beyond 1 AU have also been previously suggested [e.g., *Sarris and Malandraki*, 2003; *Lopate*, 1989; *Sarris and Krimigis*, 1985]. Therefore we suggest that traveling enhanced magnetic field regions were responsible for shaping the time intensity profiles of both ions and electrons at Cassini and thus producing this period with elevated particle intensities.

[52] The electron intensities at 1 AU from day 314 to 318 were also elevated and decaying more slowly than during the decay phase of the rest of SEP events observed during this period (Figure 4a). This period with slow decaying electron intensities occurred when the ensemble of transient solar wind flows previously observed at 1 AU were already beyond 1 AU. We suggest that both the enhanced magnetic field structures formed beyond 1 AU capable of mirroring energetic particles back to 1 AU, together with the particle injection from the backside solar events occurring from day 313 to 317 (Table 2) contributed to these elevated and slow-decaying electron intensities at 1 AU.

[53] The time-intensity profiles observed in the inner heliosphere during the October–November 2003 events were determined by both new particle injections occurring at the Sun and the formation of transient plasma structures traveling in the interplanetary medium. The highest electron intensities at Ulysses and Cassini occurred in association with the passage of enhanced magnetic field structures. The confinement and reacceleration of energetic particles within these structures made possible the observation of these events in the outer heliosphere. The highest electron intensities at 1 AU were observed during the prompt component of the SEP events and exceptionally in association with the passage of the CME-driven shock on day 302 (Table 1). The discrete nature of SEP injections, occurring at separated times and longitudes, together with the marked differences in both the characteristics of the transient structures propagating separately toward different longitudes and the various effects that these structures have on the particle populations resulted in different time-intensity profiles at each spacecraft. Therefore no periods with equal particle intensities were observed by this fleet of spacecraft.

5. Summary

[54] The main points presented in this paper are summarized as follows:

[55] 1. The series of events in October–November 2003 produced SEP events with different signatures at the heliocentric distances where they were measured. The sequence of events generated from the NOAA Active Regions 0484, 0486, and 0488 during their transit across the solar disk (and that continued once in the backside of the Sun; Table 2) produced a system of transient flows with different speeds and characteristics toward the different longitudes. The ICMEs observed at 1 AU, Ulysses, and Cassini were

associated with different solar events occurring at different times and different longitudes.

[56] 2. The system of transient flows disrupted the sequence of recurrent CIRs observed in the inner heliosphere, but it reemerged in the subsequent solar rotations.

[57] 3. The time-intensity histories of the SEP events were dominated by the passage of transient interplanetary structures. The prompt component of the SEP event associated with the fast halo CME and X17 flare on day 301 (Table 2) decreased in intensity and energy with radial distance. Whereas separated high-energy proton events where observed at 1 AU, they became merged at 5 AU. At Cassini, the highest particle intensities were observed around the passage of an enhanced magnetic field structure. At Voyager-2 the particle event was associated with the passage of a MIR.

[58] 4. The control that local interplanetary structures establish on the time-intensity profiles led to the nonobservation by two different spacecraft of a period with equal intensities.

[59] 5. Particle fluences measured throughout the duration of the event decrease with heliocentric distance slower than what is expected from adiabatic cooling in a symmetric propagating shell.

[60] 6. Particle intensities measured at Voyager-2 involved a particle population swept by the MIR, presumably formed by galactic and anomalous cosmic rays, and a population of previously shock-accelerated particles that remained confined behind the MIR-driven shock.

[61] **Acknowledgments.** We acknowledge the use of the Ulysses Data System (UDS) and the Ulysses HI-SCALE, COSPIN, SWOOPS, and VHM-FGM teams for providing the data used in this paper. We thank the ACE/SWEPAM, ACE/MAG, ACE/EPAM instrument teams and the ACE Science Center for providing the ACE data. We thank R. M. Skoug and T. H. Zurbuchen for providing ACE solar wind data collected by the SWEPAM instrument during the intense events observed from day 301 to 305 of 2003. We thank the Cassini VHM team for providing magnetic field data from this spacecraft. We thank R. B. McKibben for providing PHA data from the Ulysses COSPIN/HET instrument. The CME catalog used to identify the solar origin of the events is generated and maintained by NASA and the Catholic University of America in cooperation with the Naval Research Laboratory. SOHO is a project of international cooperation between ESA and NASA. The work at JHU/APL was supported by ACE/EPAM and Cassini/MIMI under NASA contract NAS5-97271, Ulysses/HI-SCALE under NASA research grant NAG5-6113, and Voyager/LECP under NASA research grant NNG04GN62G.

[62] Arthur Richmond thanks Christina M. S. Cohen and Robert McKibben for their assistance in evaluating this paper.

References

Balogh, A., et al. (1992), The magnetic field investigation on the Ulysses mission: Instrumentation and preliminary results, *Astron. Astrophys. Suppl. Ser.*, *92*, 221–236.

Bame, S. J., et al. (1992), The Ulysses solar wind plasma experiment, *Astron. Astrophys. Suppl. Ser.*, *92*, 237–266.

Bridge, H. S., et al. (1977), The plasma experiment on the 1977 Voyager mission, *Space Sci. Rev.*, *21*, 259–287.

Burlaga, L. F. (1975), Interplanetary streams and their interaction with the earth, *Space Sci. Rev.*, *17*, 327–352.

Burlaga, L. F., and K. W. Ogilvie (1970), Magnetic and thermal pressures in the solar wind, *Sol. Phys.*, *15*, 61–71.

Burlaga, L. F., F. B. McDonald, and R. Schwenn (1986), Formation of a compound stream between 0.85 AU and 6.2 AU and its effects on solar energetic particles and galactic cosmic rays, *J. Geophys. Res.*, *91*, 13,331–13,340.

Burlaga, L. F., et al. (2005a), Voyager 2 observations related to the October–November 2003 solar events, *Geophys. Res. Lett.*, *32*, L03S05, doi:10.1029/2004GL021480.

Burlaga, L. F., et al. (2005b), A transition to fast flows and its effects on the magnetic fields and cosmic rays observed by Voyager 2 near 70 AU, *Astrophys. J.*, *618*, 1074–1078.

Cohen, C. M. S., et al. (2005), Heavy ion abundances and spectra from the large SEP events of October–November 2003, *J. Geophys. Res.*, doi:10.1029/2005JA011004, in press.

Decker, R. B., and S. M. Krimigis (2003), Voyager observations of low-energy ions during solar cycle 23, *Adv. Space Res.*, *32*, 597–602.

de Koning, C. A., et al. (2005), An unusual fast ICME observed by Ulysses at 5 AU on November 15, 2003, *J. Geophys. Res.*, *110*, A01102, doi:10.1029/2004JA010645.

Dougherty, M. K., et al. (2004), The Cassini magnetic field investigation, *Space Sci. Rev.*, *114*, 331–383.

Dryer, M., et al. (2004), Real-time shock arrival predictions during the ''Halloween 2003 epoch'', *Space Weather*, *2*, S09001, doi:10.1029/2004SW000087.

Forsyth, R. J., A. Balogh, E. J. Smith, N. Murphy, and D. J. McComas (1995), The underlying magnetic field direction in Ulysses observations of the southern polar heliosphere, *Geophys. Res. Lett.*, *22*, 3321–3324.

Gold, R. E., et al. (1998), Electron, proton and alpha monitor on the advanced composition explorer spacecraft, *Space Sci. Rev.*, *86*, 541–562.

Irion, R. (2004), Solar physicists expose the roots of the Sun's unrest, *Science*, *305*, 600–601.

Jackman, C. M., et al. (2004), Interplanetary magnetic field at ~9 AU during the declining phase of the solar cycle and its implications for Saturn's magnetospheric dynamics, *J. Geophys. Res.*, *109*, A11203, doi:10.1029/2004JA010614.

Kallenrode, M.-B., and E. W. Cliver (2001), Rogue SEP events: Observational aspects, *Conf. Proc. 27th Int. Cosmic Ray Conf.*, *8*, 3314–3317.

Keeney, A. C. (1999), Energetic particle fluxes of two large solar events using the EPAM instrument: November 1997 and April 1998, Master's thesis, Johns Hopkins Univ., Laurel, Md.

Krimigis, S. M., et al. (1977), The Low Energy Charged Particle/LECP/ experiment on the Voyager spacecraft, *Space Sci. Rev.*, *21*, 329–354.

Krimigis, S. M., et al. (2004), Magnetosphere Imaging Instrument (MIMI) on the Cassini mission to Saturn/Titan, *Space Sci. Rev.*, *114*, 233–329.

Lanzerotti, L. J., et al. (1992), Heliosphere instrument for spectra, composition and anisotropy at low energies, *Astron. Astrophys. Suppl. Ser.*, *92*, 365–400.

Lario, D., and G. M. Simnett (2004), Solar energetic particle variations, in *Solar Variability and its Effects on Climate*, *Geophys. Monogr. Ser.*, vol. 141, edited by J. M. Pap and P. Fox, pp. 195–216, AGU, Washington, D. C.

Lario, D., et al. (2000a), Energetic proton observations at 1 and 5 AU 2. Rising phase of the solar cycle 23, *J. Geophys. Res.*, *105*, 18,251–18,174.

Lario, D., et al. (2000b), Energetic proton observations at 1 and 5 AU 1. January–September 1997, *J. Geophys. Res.*, *105*, 18,235–18,250.

Lario, D., E. C. Roelof, R. J. Forsyth, and J. T. Gosling (2001), 26-day analysis of energetic ion observations at high and low heliolatitudes: Ulysses and ACE, *Space Sci. Rev.*, *97*, 249–252.

Lario, D., E. C. Roelof, R. B. Decker, and D. B. Reisenfeld (2003), Solar maximum low-energy particle observations at heliographic latitudes above 75 degrees, *Adv. Space Res.*, *32*, 579–584.

Lario, D., S. Livi, E. C. Roelof, R. B. Decker, S. M. Krimigis, and M. K. Dougherty (2004a), Heliospheric energetic particle observations by the Cassini spacecraft: Correlation with 1 AU observations, *J. Geophys. Res.*, *109*, A09S02, doi:10.1029/2003JA010107.

Lario, D., R. B. Decker, E. C. Roelof, D. B. Reisenfeld, and T. R. Sanderson (2004b), Low-energy particle response to CMEs during the Ulysses solar maximum northern polar passage, *J. Geophys. Res.*, *109*, A01107, doi:10.1029/2003JA010071.

Lopate, C. (1989), Electron acceleration to relativistic energies by traveling interplanetary shocks, *J. Geophys. Res.*, *94*, 9995–10,010.

Lopez, R. E., D. N. Baker, and J. E. Allen (2004), Sun unleashes Halloween storm, *Eos Trans. AGU*, *85*, 105–108.

Maclennan, C. G., L. J. Lanzerotti, and S. E. Hawkins III (2001), Populating an inner heliosphere reservoir (<5 AU) with electrons and heavy ions, *Conf. Proc. 27th Int. Cosmic Ray Conf.*, *8*, 3265–3268.

Malandraki, O., et al. (2005), October/November 2003 ICMEs: ACE/EPAM solar energetic particle observations, *J. Geophys. Res.*, doi:10.1029/2004JA010926, in press.

McComas, D. J., et al. (1998), Solar wind electron proton alpha monitor (SWEPAM) for the Advanced Composition Explorer, *Space Sci. Rev.*, *86*, 563–612.

McKibben, R. B. (1972), Azimuthal propagation of low-energy solar-flare protons as observed from spacecraft very widely separated in solar azimuth, *J. Geophys. Res.*, *77*, 3957–3984.

McKibben, R. B., et al. (2003), Ulysses COSPIN observations of cosmic rays and solar energetic particles from the South Pole to the North Pole of the Sun during solar maximum, *Ann. Geophys.*, *21*, 1217–1228.

McKibben, R. B., et al. (2005), Energetic particle observations from the Ulysses COSPIN instruments obtained during the October–November 2003 events, *J. Geophys. Res.*, doi:10.1029/2005JA011049, in press.

Neugebauer, M., and R. Goldstein (1997), Particle and field signatures of coronal mass ejections in the solar wind, in *Coronal Mass Ejections*, *Geophys. Monogr. Ser.*, vol. 99, edited by N. Crooker, J. A. Joselyn, and J. Feynman, pp. 245–251, AGU, Washington, D. C.

Richardson, I. G. (1997), Using energetic particles to probe the magnetic topology of ejecta, in *Coronal Mass Ejections*, *Geophys. Monogr. Ser.*, vol. 99, edited by N. Crooker, J. A. Joselyn, and J. Feynman, pp. 189–198, AGU, Washington, D. C.

Richardson, J. D., C. Wang, and J. C. Kasper (2005), Propagation of the October/November 2003 CMEs through the heliosphere, *Geophys. Res. Lett.*, *32*, L03S03, doi:10.1029/2004GL020679.

Roelof, E. C., R. E. Gold, G. M. Simnett, S. J. Tappin, T. P. Armstrong, and L. J. Lanzerotti (1992), Low-energy solar electron and ions observed at Ulysses February–April 1991: The inner heliosphere as particle reservoir, *Geophys. Res. Lett.*, *19*, 1243–1246.

Sanderson, T. R., R. Reinhard, P. van Nes, and K.-P. Wenzel (1985), Observations of three-dimensional anisotropies of 35- to 1000-keV protons associated with interplanetary shocks, *J. Geophys. Res.*, *90*, 19–27.

Sarris, E. T., and S. M. Krimigis (1985), Quasi-perpendicular shock acceleration of ions to ~200 MeV and electrons to ~2 MeV observed by Voyager-2, *Astrophy. J.*, *298*, 676–683.

Sarris, E. T., and O. E. Malandraki (2003), Dependence of the decay phase of solar energetic electron events on the large scale IMF structure: ACE observations, *Geophys. Res. Lett.*, *30*(21), 2079, doi:10.1029/2003GL017921.

Sauer, H. H. (1993), GOES observations of energetic protons E > 685 MeV: Description and data comparison, *Conf. Proc. 23rd Int. Cosmic Ray Conf.*, *3*, 250–253.

Shea, M. A., and D. F. Smart (2001), Solar proton and GLE event frequency: 1955–2000, *Conf. Proc. 27th Int. Cosmic Ray Conf.*, *8*, 3401–3404.

Simpson, J. A., et al. (1992), The Ulysses cosmic ray and solar particle investigation, *Astron. Astrophys. Suppl. Ser.*, *92*, 401–410.

Skilling, J. (1975), Cosmic ray streaming. I - Effect of Alfven waves on particles, *Mon. Not. R. Astron. Soc.*, *172*, 557–566.

Skoug, R. M., et al. (2004), Extremely high speed solar wind: 29–30 October 2003, *J. Geophys. Res.*, *109*, A09102, doi:10.1029/2004JA010494.

Smith, C. W., et al. (1998), The ACE magnetic field experiment, *Space Sci. Rev.*, *86*, 613–632.

Woods, T. N., et al. (2004), Solar irradiance variability during the October 2003 solar storm period, *Geophys. Res. Lett.*, *31*, L10802, doi:10.1029/2004GL019571.

R. B. Decker, S. M. Krimigis, D. Lario, S. Livi, and E. C. Roelof, Johns Hopkins University Applied Physics Laboratory, 11100 Johns Hopkins Road, Laurel, MD 20723, USA. (rob.decker@jhuapl.edu; tom.krimigis@jhuapl.edu; david.lario@jhuapl.edu; stefano.livi@jhuapl.edu; edmond.roelof@jhuapl.edu)

C. D. Fry, Exploration Physics International, Inc., Suite 37-105, 6275 University Drive, Hunstville, AL 35806-1776, USA. (gfry@expi.com)

C. T. Russell, Department of Earth and Space Sciences, Institute of Geophysics and Planetary Physics, University of California, Los Angeles, 3845 Slichter Hall, MS 156704, 405 Hilgard Avenue, Los Angeles, CA 90095-1567, USA. (ctrussel@igpp.ucla.edu)